LOAN DOCUMENT

PHOTOGRAPH THIS SHEET

DTIC ACCESSION NUMBER

LEVEL

0

INVENTORY

WL-TR-96-2084

DOCUMENT IDENTIFICATION

DISTRIBUTION STATEMENT A
Approved for public release
Distribution Unlimited

DISTRIBUTION STATEMENT

HANDLE WITH CARE

ACCESSION FOR		
NTIS	GRA&I	☑
DTIC	TRAC	☐
UNANNOUNCED		☐
JUSTIFICATION		
BY		
DISTRIBUTION/		
AVAILABILITY CODES		
DISTRIBUTION	AVAILABILITY AND/OR SPECIAL	
A-1		

DISTRIBUTION STAMP

DATE ACCESSIONED

DTIC QUALITY INSPECTED 1

DATE RETURNED

A-1

19960812 166

DATE RECEIVED IN DTIC

REGISTERED OR CERTIFIED NUMBER

PHOTOGRAPH THIS SHEET AND RETURN TO DTIC-FDAC

DTIC FORM JUN 90 70A

DOCUMENT PROCESSING SHEET

PREVIOUS EDITIONS MAY BE USED UNTIL STOCK IS EXHAUSTED.

LOAN DOCUMENT

WL-TR-96-2084

TRANSITION ON TURBINE BLADES AND CASCADES AT LOW REYNOLDS NUMBERS

Richard B. Rivir

June 17-20, 1996

FINAL REPORT 1 NOVEMBER 1995--9 JULY 1996

Approved for public release; distribution unlimited

AERO PROPULSION & POWER DIRECTORATE
WRIGHT LABORATORY
AIR FORCE MATERIEL COMMAND
WRIGHT-PATTERSON AIR FORCE BASE, OH 45433-7650

NOTICE

WHEN GOVERNMENT DRAWINGS, SPECIFICATIONS, OR OTHER DATA ARE USED FOR ANY PURPOSE OTHER THAN IN CONNECTION WITH A DEFINITELY GOVERNMENT-RELATED PROCUREMENT, THE UNITED STATES GOVERNMENT INCURS NO RESPONSIBILITY OR ANY OBLIGATION WHATSOEVER. THE FACT THAT THE GOVERNMENT MAY HAVE FORMULATED OR IN ANY WAY SUPPLIED THE SAID DRAWINGS, SPECIFICATIONS, OR OTHER DATA, IS NOT TO BE REGARDED BY IMPLICATION, OR OTHERWISE IN ANY MANNER CONSTRUED, AS LICENSING THE HOLDER, OR ANY OTHER PERSON OR CORPORATION; OR AS CONVEYING ANY RIGHTS OR PERMISSION TO MANUFACTURE, USE, OR SELL ANY PATENTED INVENTION THAT MAY IN ANY WAY BE RELATED THERETO.

THIS REPORT IS RELEASABLE TO THE NATIONAL TECHNICAL INFORMATION SERVICE (NTIS). AT NTIS, IT WILL BE AVAILABLE TO THE GENERAL PUBLIC, INCLUDING FOREIGN NATIONS.

THE TECHNICAL REPORT HAS BEEN REVIEWED AND IS APPROVED FOR PUBLICATION.

Richard B. Rivir

RICHARD B. RIVIR
Manager, Aerothermal Research
Turbine Branch
Turbine Engine Division
Aero Propulsion & Power Directorate

Charles D. MacArthur

CHARLES D. MACARTHUR
Chief
Turbine Branch
Turbine Engine Division
Aero Propulsion & Power Directorate

Richard J. Hill

RICHARD J. HILL
Chief of Technology
Turbine Engine Division
Aero Propulsion & Power Directorate

IF YOUR ADDRESS HAS CHANGED, IF YOU WISH TO BE REMOVED FROM OUR MAILING LIST, OR IF THE ADDRESSEE IS NO LONGER EMPLOYED BY YOUR ORGANIZATION PLEASE NOTIFY WL/POTT, WPAFB OH 45433-7650 TO HELP MAINTAIN A CURRENT MAILING LIST.

REPORT DOCUMENTATION PAGE

Form Approved OMB No. 0704-0188

1. AGENCY USE ONLY *(Leave blank)*

2. REPORT DATE
JUNE 17-20, 1996

3. REPORT TYPE AND DATES COVERED
Final 1 Nov 95 - 9 Jul 96

4. TITLE AND SUBTITLE
TRANSITION ON TURBINE BLADES AND CASCADES AT LOW REYNOLDS NUMBERS

5. FUNDING NUMBERS
PE 61102F
JON 2307S315

6. AUTHOR(S)
Richard B. Rivir

7. PERFORMING ORGANIZATION NAME(S) AND ADDRESS(ES)
Aero Propulsion & Power Directorate
Wright Laboratory
Air Force Materiel Command
Wright-Patterson Air Force Base, OH 45433-7650

8. PERFORMING ORGANIZATION REPORT NUMBER

9. SPONSORING/MONITORING AGENCY NAME(S) AND ADDRESS(ES)
Aero Propulsion & Power Directorate
Wright Laboratory
Air Force Materiel Command
Wright-Patterson Air Force Base, OH 45433-7650
POC: Richard B Rivir, WL/POTT, 513-255-5132

10. SPONSORING/MONITORING AGENCY REPORT NUMBER
WL-TR-96-2084

11. SUPPLEMENTARY NOTES
AIAA 96-2079 TRANSITION ON TURBINE BLADES AND CASCADES AT LOW REYNOLDS NUMBERS
27th AIAA FLUID DYNAMICS CONFERENCE, June 17-20, 1996, New Orleans LA

12a. DISTRIBUTION/AVAILABILITY STATEMENT
APPROVED FOR PUBLIC RELEASE; DISTRIBUTION IS UNLIMITED

12b. DISTRIBUTION CODE

13. ABSTRACT *(Maximum 200 words)*

Unpredicted losses in the low pressure turbine during operation at high altitudes has stimulated current interest in transition, and separation at low Reynolds numbers. In the turbine, free stream turbulence levels or unsteadiness resulting from vane wakes, passage vorticies, and end wall horseshoe vorticies exceeds the unsteadiness levels associated with a fully turbulent boundary layer. Transition and transition length are found to be a function of both turbulence intensity and length scale although there are no empirical relationships to be found in the literature which include both. An experimental and computation effort was undertaken to investigate the effect of turbulence intensity, and turbulence length scale on transition location, and transition length scale on transition location, and transition length in a Langston turbine cascade for solidities of 1.075 and 0.84 at Reynolds numbers of 50K to 2000K. Experimental observations of transition at turbulence levels of 1 and 10% for three integral turbulence scales indicate a relative lack of sensitivity to turbulence level and scale for the momentum thickness transition location, but a sensitivity to both for transition length.

14. SUBJECT TERMS

15. NUMBER OF PAGES
16

16. PRICE CODE

17. SECURITY CLASSIFICATION OF REPORT	18. SECURITY CLASSIFICATION OF THIS PAGE	19. SECURITY CLASSIFICATION OF ABSTRACT	20. LIMITATION OF ABSTRACT
UNCLASSIFIED	UNCLASSIFIED	UNCLASSIFIED	SAR

GENERAL INSTRUCTIONS FOR COMPLETING SF 298

The Report Documentation Page (RDP) is used in announcing and cataloging reports. It is important that this information be consistent with the rest of the report, particularly the cover and title page. Instructions for filling in each block of the form follow. It is important to ***stay within the lines*** to meet ***optical scanning requirements***.

Block 1. Agency Use Only *(Leave blank)*.

Block 2. Report Date. Full publication date including day, month, and year, if available (e.g. 1 Jan 88). Must cite at least the year.

Block 3. Type of Report and Dates Covered. State whether report is interim, final, etc. If applicable, enter inclusive report dates (e.g. 10 Jun 87 - 30 Jun 88).

Block 4. Title and Subtitle. A title is taken from the part of the report that provides the most meaningful and complete information. When a report is prepared in more than one volume, repeat the primary title, add volume number, and include subtitle for the specific volume. On classified documents enter the title classification in parentheses.

Block 5. Funding Numbers. To include contract and grant numbers; may include program element number(s), project number(s), task number(s), and work unit number(s). Use the following labels:

C	- Contract	**PR**	- Project
G	- Grant	**TA**	- Task
PE	- Program Element	**WU**	- Work Unit Accession No.

Block 6. Author(s). Name(s) of person(s) responsible for writing the report, performing the research, or credited with the content of the report. If editor or compiler, this should follow the name(s).

Block 7. Performing Organization Name(s) and Address(es). Self-explanatory.

Block 8. Performing Organization Report Number. Enter the unique alphanumeric report number(s) assigned by the organization performing the report.

Block 9. Sponsoring/Monitoring Agency Name(s) and Address(es). Self-explanatory.

Block 10. Sponsoring/Monitoring Agency Report Number. *(If known)*

Block 11. Supplementary Notes. Enter information not included elsewhere such as: Prepared in cooperation with...; Trans. of...; To be published in.... When a report is revised, include a statement whether the new report supersedes or supplements the older report.

Block 12a. Distribution/Availability Statement. Denotes public availability or limitations. Cite any availability to the public. Enter additional limitations or special markings in all capitals (e.g. NOFORN, REL, ITAR).

DOD - See DoDD 5230.24, "Distribution Statements on Technical Documents."
DOE - See authorities.
NASA - See Handbook NHB 2200.2.
NTIS - Leave blank.

Block 12b. Distribution Code.

DOD - Leave blank.
DOE - Enter DOE distribution categories from the Standard Distribution for Unclassified Scientific and Technical Reports.
NASA - Leave blank.
NTIS - Leave blank.

Block 13. Abstract. Include a brief *(Maximum 200 words)* factual summary of the most significant information contained in the report.

Block 14. Subject Terms. Keywords or phrases identifying major subjects in the report.

Block 15. Number of Pages. Enter the total number of pages.

Block 16. Price Code. Enter appropriate price code *(NTIS only)*.

Blocks 17. - 19. Security Classifications. Self-explanatory. Enter U.S. Security Classification in accordance with U.S. Security Regulations (i.e., UNCLASSIFIED). If form contains classified information, stamp classification on the top and bottom of the page.

Block 20. Limitation of Abstract. This block must be completed to assign a limitation to the abstract. Enter either UL (unlimited) or SAR (same as report). An entry in this block is necessary if the abstract is to be limited. If blank, the abstract is assumed to be unlimited.

Transition on Turbine Blades and Cascades at Low Reynolds Numbers

Richard B. Rivir*
Aero Propulsion and Power Directorate
US Air Force Wright Laboratory
Wright Patterson AFB, Ohio

Abstract

Unpredicted losses in the low pressure turbine during operation at high altitudes has stimulated current interest in transition, and separation at low Reynolds numbers. In the turbine, free stream turbulence levels or unsteadiness resulting from vane wakes, passage vorticies, and end wall horseshoe vorticies exceeds the unsteadiness levels associated with a fully turbulent boundary layer. Transition and transition length are found to be a function of both turbulence intensity and length scale although there are no empirical relationships to be found in the literature which include both. An experimental and computation effort was undertaken to investigate the effect of turbulence intensity, and turbulence length scale on transition location, and transition length in a Langston turbine cascade for solidities of 1.075 and 0.84 at Reynolds numbers of 50K to 2000K. Experimental observations of transition at turbulence levels of 1 and 10% for three integral turbulence scales indicate a relative lack of sensitivity to turbulence level and scale for the momentum thickness transition location, but a sensitivity to both for transition length.

Nomenclature

Bx	x projected turbine blade chord (m)
C	turbine blade chord (m)
c_μ	Turbulent coefficient of viscosity
K	acceleration parameter$(U^2/\nu)\partial U/\partial x$ $(1/s^2)$
p	turbine blade pitch (m)
s	surface distance on turbine blade (m)
Re_θ	Reynolds number based on momentum thickness
$Re_{\theta s}$	Reynolds number based on momentum thickness at separation
Re_{ltr}	Reynolds number based on transition length
Re_{st}	Reynolds number based on a transition after separation
t'	rms component of temperature (°/s)
Tu	turbulence intensity (u'/U)
u'	rms component of x velocity (m/s)
U	x component of velocity (m/s)
v'	rms component of y velocity (m/s)
Λ_I	Integral scale of turbulence (m)
λ_μ	micro scale of turbulence (m)
λ_θ	acceleration parameter $(-\theta^2/\nu)\partial U/\partial x$
θ	momentum thickness (m)

Introduction

The commonly held physical picture of the transition process is illustrated schematically in Figure 1. Two D Tollimien Schlicting waves are amplified, breaking down into Emmons spots which propagate as a wedge with a following quiet wedge region until the boundary layer has become fully turbulent. Turbine transitions normally will bypass the Tollimien Schlicting part of the process and break down directly as a result of the high levels of unsteadiness present. A laminar separation with transition in the separation bubble, as is also illustrated in Figure 1, is not an uncommon mode of turbine transition since turbines must operate over a wide range of conditions which include large

* Associate Fellow

changes in angles of incidence, Re, and inlet distortions.

Mayle's 1991 review paper provided the most recent comprehensive look at the transition problems in turbine engines. There has been no shortage of transition papers as well since Mayle's work. Walker, 1993 and Roshoko, 1994 have published subsequent surveys. Additional surveys can be found in Euromech 327, Ercoftac Bulletin March 1995, AGARD CP-551 Application of Direct and Large Eddy Simulation to Transition and Turbulence 1994, and the Syracuse University Minnowbrook Work Shop on End Stage Boundary Layer Transition, 1993.

Mayle's paper provided a compilation of useful empirical relationships and data for Tu levels below 8%. Bypass transition is the primary mechanism of interest in turbine related flows due to the high levels of unsteadiness - although all transition mechanisms can exist at different times at the same location on a blade. According to Mayle deficiencies that existed in 1991 included a lack of u'v' and v't' measurements, virtually no measured turbulence length scales at transition, and scarce transition measurements in accelerating and decelerating flows.

Since 1991, Zhou and Wang 1993 measured u'v' and v't' in a zero pressure gradient and in a favorable pressure gradient, transitioning flat plate flow with grid generated turbulence up to 6.4%. They observed large changes in the spot formation rate with the acceleration parameter K. The turbulent spot formation decreased by an order of magnitude at the higher turbulence levels with a doubling of the acceleration parameter.

Volino and Simon, 1995 provided detailed measurements of transitional boundary layers on concave surfaces with Tu up to 8%. The production of wall disturbances began transition when K was less than 2×10^{-6}. For strong acceleration, $K > 3\times10^{-6}$, they found that the intermittancy became nearly constant and transition was inhibited. However even at the highest value of their acceleration parameter, $K=9\times10^{-6}$ and Tu=8%, there still was an extended transitional region which was dominated by the free stream scales with fluctuations in heat transfer and skin friction between fully turbulent and laminar. Under these conditions the transition became intermittent, with Tu dropping from 8% to 1.6% through the acceleration region. As Tu dropped to 1.6% the favorable acceleration took over dominating and suppressing any tendency to transition.

Simon, 1995 gave two empirical relationships for the variation of transition length with momentum thickness Re and suggested, as did Mayle, that additional experimental data is needed. Walker, 1993, also addressed transition length suggesting that K is an inappropriate parameter, and that if one chooses $\lambda_\theta = (\theta^2/\nu)dU/dx$ as the acceleration parameter, the effect of acceleration may be included in the transition length relationship.

Laminar separation with a subsequent transition, as illustrated in Figure 1, can and does occur on turbine blades. Walker suggests $R_{est}=700R_{e\theta}s^{0.7}$ in laminar separation bubbles. Measurements of transition in separation bubbles are difficult and very scarce. There remain many uncertainties in the recovery region of separation bubbles as to whether transition has been completed or not, as well as to exactly which parameters and characterizations are relevant for transition in laminar separated flows.

Since modern turbine blades have high aft loading transition location, transition length, and flow separation have a significant influence on their performance. C-17(F-117) engines as well as smaller engines with their associated smaller blades typically exhibit higher than predicted SFC during high altitude operation. The additional operational loss in SFC can amount to 0.8% over design calculations. The current inability to accurately predict the transition, separation, and reattachment at low Reynolds numbers in turbines is associated with the high levels of turbulence and unsteadiness of the flow. A low pressure turbine typically operates at a chord Reynolds number of 10^6 at take off. The chord Reynolds number falls to 10^5 at altitude in a number of engines. Sharma, 1994, reported a near doubling of the measured loss coefficient, as illustrated in Figure 2, from cascade measurements, when the chord Reynolds number is reduced from 300K to 50K.

In our work on low pressure, low Reynolds number turbine flows we have a few new measurements of transition, transition length and turbulence scales to add to the above picture for the free stream turbulence levels of 1 and 10%. The experimental measurements have been performed in a Langston cascade with two pitch to chord ratios and three turbulence scales. Computations using the Allision Blade Vane Interaction program, a 2 D Navier-Stokes solver, for two pitch to chord ratios and six chord Reynolds numbers have also been carried out and will be compared to the experimental measurements.

Low Reynolds Number Cascade

A Combined experimental and computational study was conducted to investigate transition over the suction surface of a low Reynolds number turbine cascade to determine how it is affected by freestream turbulence intensity, freestream turbulence scale, and solidity (C/p). The Langston cascade, Langston et al., 1977, was chosen as the geometry for investigation since it is a well documented geometry at higher Reynolds numbers, while still fairly representative of current low pressure turbine geometries. Two similar experimental cascades were used, one at the Air Force Academy and one at UC Davis, the documentation of both will be found in Baughn et al., 1995. The nominal cascade chord is 17.1cm and the aspect ratio 3.9. The investigation spanned a range of solidities of 0.084 to 1.075, turbulence levels from 0.5% to 10%, and integral turbulence scales from .0054m to 0.0704m. Computations for two of the experimental solidity ratios (C/p=0.84 and 1.075) have been carried out at six chord Reynolds numbers (50K, 100K, 200K, 441K, 1,000K, and 2,000K.

Computational Results

The computational code used for the numerical simulation of the steady Navier-Stokes equations was the VBI code developed by the Allison engine company, Rao et al., 1994, under U.S. Air Force contract. The steady state solution of the code is based on a five step Runge Kutta relaxation method that incorporates residual smoothing to accelerate convergence to the final solution. The code implements a Baldwin-Lomax, 1978, two-layer algebraic turbulence model and the Baldwin-Lomax transition point model. There is no transition length associated with this turbulence model, transition occurs at the fixed recommended value of the turbulent viscosity coefficient, c_μ=14, which corresponds to $R_{e\theta}$=300-419. The grid used in this code is an overlaid combination of a rectangular H grid and a body fitted hyperbolic O grid. The rectangular grid is used to resolve the free stream flow and the O grid is used to resolve the regions of high shear associated with the boundary layer. Small values of y+ have been employed in the calculation for the O grid spacing, with the first grid point at a y+ of 1 or less.

The computational results presented in Figures 3 through 5 demonstrate the effect of chord Re on the computed boundary layer characteristics on the blade suction surface for two solidities. Figure 3 and 4 show typical $R_{e\theta}$ variations over the blade suction surface at a chord Re of 50K for the two solidities of 0.84 and 1.075 respectively. In the first case (C/p=0.84) the suction surface boundary layer undergoes transition at the computed $R_{e\theta}$=310 followed by separation and then laminar reattachment. When the solidity is increased to, C/p=1.075 (Figure 4), the boundary layer over the suction surface undergoes laminar separation (as illustrated schematically in Figure 1) before transition at $R_{e\theta}$ =347 and turbulent reattachment near the trailing edge. The computed transition locations for the two chord to solidities at six Reynolds numbers ranging from 50K to 2000K is presented in Figure 5. The results indicate that in general the transition location moves forward as Reynolds number increases. The transition location occurs earlier for the low solidity case, however these flows were found to suffer severe flow separations. Depending on the solidity, the entire suction surface boundary layer becomes turbulent above a chord Re of 1000K for C/p=1.075, and above 100K for C/p=0.84. The complete results including separation and reattachment calculations for these flows can be found in Rivir et al., 1996. These results will next be compared with the experimental low (1%) freestream turbulence case.

Experimental Measurements of Low Reynolds Number Transition

Experimental measurements for transition location and transition length were obtained at low Reynolds numbers (64K-144K) in the Langston Cascade for solidities ranging from 0.084 to 1.075. The location of the transition, separation, and reattachment points were determined by a narrow band liquid crystal which was applied to a vapor deposited gold heated film on the surface of the cascade airfoil. Turbulence (Tu=0.5, 1, and 10%) was generated by square mesh grids which were nominally located > 25 mesh distances upstream, so that turbulence was in the final period of decay and slowly changing with x. The integral scale of turbulence (0.005m to 0.0704m) was measured by autocorrelation of the hot wire signal along with Taylor's Hypothesis. The micro scale was obtained from $1/\lambda_\mu=-1/U(\partial^2R(T)/\partial T^2)$ applied to the autocorrelation function R(T) of the hot wire's signal. Three square mesh turbulence grids were employed, all of which generate 10% freestream levels of Tu. The grid generated turbulence scale characteristics investigated are tabulated in Table 1.

Also presented on Figure 5 are the experimentally measured transition locations at a chord Re of 67K (C/p=1.075)and 110K (C/p=0.84)at Tu=1%. The agreement with the computational results for the two solidities is excellent. The C/p=0.84 experimental case was observed to relaminarize and then transition again at a s/Bx of 0.93.

Effect of Turbulence Intensity

Transition Location $R_{e\theta t}$

Figure 6 shows Mayle's empirical relationship for $R_{e\theta t}$ dependence on Tu with the original data he used which indicates increased $R_{e\theta t}$ with increasing Tu scale. Figure 6 also includes three additional sets of data that were not included in Mayle's paper The first set represents Zhou and Wang's 1993 measurements in zero and favorable pressure gradient transitioning flat plate flows. These results were obtained at grid generated turbulence levels of 0.5 to 6.4% and turbulence scales of 1.8 to 2.8cm, showing excellent agreement with Mayle's correlation. Zhou and Wang also added acceleration with only a small resulting increase (110 to 130) in $R_{e\theta t}$. Mayle's value at 2.2% Tu for $K=0.75*10^{-6}$, was 244. The second and third sets correspond to experimental measurements in the Langston cascade and Dring's rotating Langston cascade. The second set represents the experimental results from Baughn et al., 1995 which were obtained at Tu=1% and 10% in the Langston cascade. In these experiments surface heat transfer measurements were used to determine the transition locations, s/Bx. The computational results from Rivir et al., 1996 were then used to deduce the value of $R_{e\theta t}$ based upon the measured experimental transition locations. The Tu=1% points correspond well to the empirical relationship while the Tu=10% points show a much larger value (5x) for $R_{e\theta t}$ than the empirical relationship. The third data point shown on Figure 6 is from Dring et al., 1986 rotating low Re Langston cascade (see Table 1). Again the empirical prediction under predicts the $R_{e\theta t}$ by a factor of two. The rotating and 10% cascade data show the general trend with scale but are not accurately captured by the empirical models.

Transition Length

The experimentally measured surface heat transfer data in the low Re Langston cascade are presented in Figure 7 for turbulence levels of 1% and 10%. Figure 7 illustrates the effect of turbulence intensity on the apparent length of transition, comparing the Tu=1% and the Tu=10% data, at nominally the same Re, we see transition moves forward with increasing Tu and the length of the transition increases. Figure 8 presents two empirical relationships for the R_{elt} dependence from Simon. The two correlations are $R_{elt}=124*R_{e\theta tr}{}^{3/2}$ for a zero pressure gradient, and $R_{elt}=344*R_{e\theta tr}{}^{3/2}$ for a weak pressure gradient ($K=0.75*10^{-6}$). Lacking an exact measurement of velocity at transition the range of velocities was determined based upon the cascade entrance and exit velocities. The range of transition lengths from the experimental measurements indicate transition length Reynolds numbers of 20K to 83K. Using the calculated values of $R_{e\theta t}$, as explained in the previous section, the cascade experiments at low Reynolds numbers fall near the zero pressure gradient relation, $124*R_{e\theta tr}{}^{3/2}$. Although we have not yet measured $R_{e\theta}$ directly it is clearly much larger for the cascade from comparison of s/Bx at transition in Table 1 than obtained in Dring's rotating test of the Langston cascade.

Combining Mayle's $Re_{\theta t}=400Tu^{-5/8}$ with Simon's above relationships gives Figure 9 for the two Simons curves, the third curve is a similar relation from Mayle with $\theta e=\theta t$. Both the high turbulence (Tu=10%) data for the cascade as well as Dring's 1986 low Re rotating data fall well below Simon's upper curve which is for small acceleration($K=0.75*10^{-6}$). The acceleration at transition for the Langston cascade is calculated to be on the order of $3*10^{-5}$, at Re=50K, an order of magnitude higher. The low Re data therefore should have fallen above the top curve if the top curve was also applicable for strong accelerations. Here one should heed Volino and Simon's observation that typical turbine blade accelerations virtually shut of boundary layer turbulence generation. The 1% Tu case is also shown on Figure 9 and is 1 to 2 orders of magnitude below Mayle's and Simon's correlations respectively. This would indicate that this relationship with Tu may also be much flatter than current empirical models predict. A common assumption used is that the velocity fluctuations are frozen through the blade passage so turbulence is expected to change along the blade suction and pressure surfaces as the freestream velocity varies and like wise the turbulence at transition will be significantly less than at the cascade entrance. Revised empirical relationships are required to accurately describe the low pressure, low Re turbine flows.

Effect of Turbulence Scale

The characteristics of the three turbulence grids employed in the low Re turbine cascade experiment are listed in Table 1 along with the corresponding locations of transition and transition lengths. The experimentally measured location of transition by Sharp and Harris, 1996 is shown in Figure 10 for two grids and the clean tunnel (Λ_f=0.0704m, Λ_f=0.0132m, Λ_f=0.0054m) at chord Re's of 76.7K and 79.9K. The transition location s/Bx moved forward, as turbulence increased from 0.5% to 10%. The forward movement in s/Bx is in this case small. Both grids produced 10% turbulence intensities at the cascade face and both resulted in transition at the same value of s/Bx. The transition length was significantly altered with the larger scale increasing the length by 30% as seen in Figure 10.

It has not been established whether the transition is complete at the trailing edge of our Langston cascade blade. The electrodes for the gold foil surface are located at the trailing edge creating a small discontinuity in the heat flux per unit area which may be altering the trailing edge observations. The observed heat transfer level at the trailing edge is flattened and appears to be in between laminar and turbulent for the transitioning cases investigated. It remains to be determined with detailed velocity profiles whether the transition is complete at the trailing edge or still under development and unsteady. The resulting freestream Tu level and Tu scales should be documented during transition for accelerating turbine cascade flows. These determinations would of course influence the interpretation of transition length, but even more important the state of the boundary layer in this flat region and its implication on losses.

Figure 11 presents the results for all three grids investigated relating the integral scale of turbulence to transition location and transition length. The location does not change significantly over the range of integral scales investigated. The length of transition does how ever increase slightly with an increase in scale. Dring's rotating data again is indicated for comparison and we see comparable transition lengths but a significantly forward transition location or $R_{e\theta t}$.

Summary

The Low Reynolds number computations in the Langston cascade show oscillating transition, separation and reattachments. The experimental cascade measurements indicate weak $R_{e\theta t}$ dependency on with turbulence intensity for the turbulence scales investigated. The calculations showed good agreement with the experiment for both C/p ratio of 1.075 and 0.84 for Tu=1%. Both our experiments and our calculations show strong effects of the solidity on the transition length and the tendency towards laminar separation (with subsequent transition) at low solidities. Although we are still lacking detailed velocity profiles at transition for the Langston cascade, it would appear that the acceleration parameter K does not influence turbulence intensity's effect on transition length to the same degree observed in flat plate experiments. The effects of turbulence scale on transition were also found to be modified in the cascade. At 10% freestream turbulence the $R_{e\theta t}$ and x location of transition was unaffected by turbulence scale. The transition length however increased by 30% when the turbulence scale increased decreased by 81%.

The comparison with the rotating Langston turbine indicates that $R_{e\theta t}$ is modified by rotation significantly while the transition length is unaffected. Turbulence scale effects in both cascades and rotating experiments appear to significantly alter the current empirical flat plate relationships.

Acknowledgments

Rolf Sondergaard of Wright Laboratory, James Baughn of UC Davis, Aaron Byerley of Mercer University, Capt Robert Butler, Lt Col Ken VanTreuren, Lt Col Neal Barlow, C1C Jason Sharp, and C2C Pete Harris of the U.S. Air Force Academy have all made significant contributions to the low Reynolds number low pressure turbine results presented.

References

"Application of Direct and Large Eddy Simulation to Transition and Turbulence", December 1994, AGARD-CP-551.

"European Research Community On Flow Turbulence and Combustion" Bulletin, March 1995.

Baldwin, B. S., and Lomax, H., 1978, "Thin-Layer Approximation and Algebraic Model for Separated Turbulent Flows," AIAA Paper 78-0257.

Baughn, J. W., Butler, R. J., Byerley, A. R., and Rivir R. B., August 1995, "An Experimental Investigation of Heat Transfer, Transition and Separation On Turbine Blades at Low Reynolds Number and High Turbulence Intensity," 1995 ASME International Mechanical Engineering Congress and Exposition.

Dring, R. P., Blair, M. F., and Joslyn, H. D., 1986, "The Effects of Inlet Turbulence and Rotor Stator Interactions on the Aerodynamic and Heat Transfer of a Large Scale Rotating Turbine Model, Volume 11-Heat Transfer Data Tabulation, 15% Axial Spacing," NASA CR 179467, UTRC-R86-956480-2.

Langston, L. S., Nice, M. L., and Hopper, R. M., 1977, "Three Dimensional Flow within a Turbine Cascade Passage," *Journal for Engineering and Power*, Vol. 99, pp. 21-28.

LaGraff, J.E., 1993, "Syracuse University Minnowbrook Workshop on End-Stage Boundary Layer Transition".

Mayle, R.E., 1991, "The Role of Laminar-Turbulent Transition in Gas Turbine Engines", ASME paper 91-GT-282.

Reshotko, E., 1994, "Boundary Layer Instability, Transition and Control", AIAA paper 94-0001.

Sharma, O., P., Ni, R.H., and Tanrikut, S., 1994, Turbomachinery Design Using CFD. "Unsteady Flows in Turbines--Impact on Design Procedure", AGARD-LS-195, Paper No. 5.

Sharp, J. and Harris, P., 1996, "Turbulent Heat Transfer Investigation: Turbulence Length Scales and Turbine Heat Transfer", United States Air Force Academy, Aeronautical Engineering 471 Report.

Simon, F.F., 1994, "The Use of Transition Region Characteristics to Improve the Numerical Simulation of Heat Transfer in Bypass Transitional Flows", NASA TM 106445.

Rao, K. V., Delaney, R. A., and Dunn M. G., "Vane-Blade Interaction in a Transonic Turbine, Part 1 Aerodynamics," May-June 1994, *Journal of Propulsion and Power*, Vol. 10 No. 3, pp. 305-311.

Rivir, R., Sondergaard R., Dalhstrom M., and Ervin E., "Low Reynolds Number Turbine Blade Cascade Calculations," Feburary 1996, ISROMAC-6 The 6th International Symposium on Transport Phenomena and Dynamics of Rotating Machinery, Honolulu, HA.

Roberts, W.B., 1980, "Calculation of Laminar Separation Bubbles and their Effect on Airfoil Performance," AIAA Journal, Vol. 18 pp 25-31.

Volino, R.J., and Simon, T.W., 1995, "Measurements in Transitional Boundary Layers Under High Free-Stream Turbulence and Strong Acceleration Conditions," NASA CR 198413.

Walker, G.J., 1975, "Observations of Separated Laminar Flow on Axial Turbomachine Blading,"AIAA Journal, Vol. 27, pp 595-602.

Walker, G.J., 1993, "The Role of Laminar-Turbulent Transition in Gas Turbine Engines: A Discussion", ASME Journal of Turbomachinery, Vol. 115, pp 207-217.

White F.M., 1974, Viscous Fluid Flow, McGraw-Hill, New York, NY.

Zhou, D., and Wang, T., 1993, "Effects of Elevated Free-Stream Turbulence and Streamwise Acceleration on Flow and Thermal Structures in Transitional Boundary Layers", Final Report, Office of Naval Research, Grant No. N00014-89-J-3105.

Table 1 Grid, Turbulence Scale Characteristics

Re	Λ_I (m)	λ_μ (m)	Tu%	s/Bx_t	L_t/Bx	Reference
67K	0.006		0.5	0.25,0.9	0.25	Baughn et al., 1995
76.7	0.0054		0.5	1.113	0.297	Sharp and Harris, 1966
79.9K	0.0132	0.005	10	0.964	0.297	Sharp and Harris, 1966
134K	0.0404	0.006	10	1.0	0.5	Baughn et al., 1995
76K	0.0704	0.008	10	0.983	0.537	Sharp and Harris, 1996
134K	0.0203	0.002	9.8	0.4	0.4	Dring et al., 1986

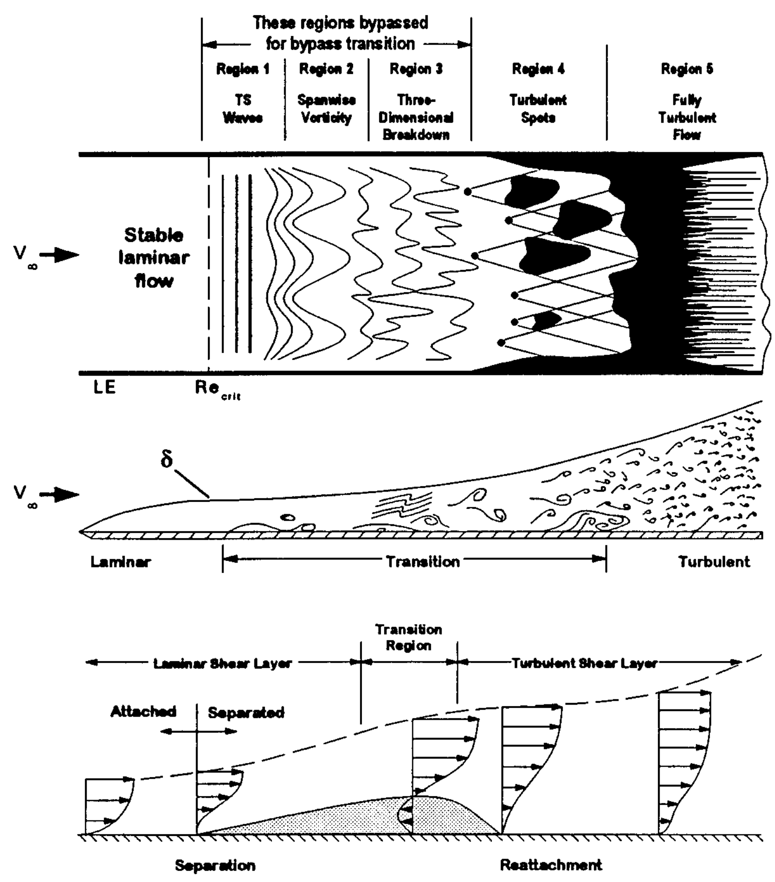

Figure 1. Schematics of the Transition Process / Schematic of Laminar Separation with Transition (White, 1974 / Walker, 1975, and Roberts, 1990)

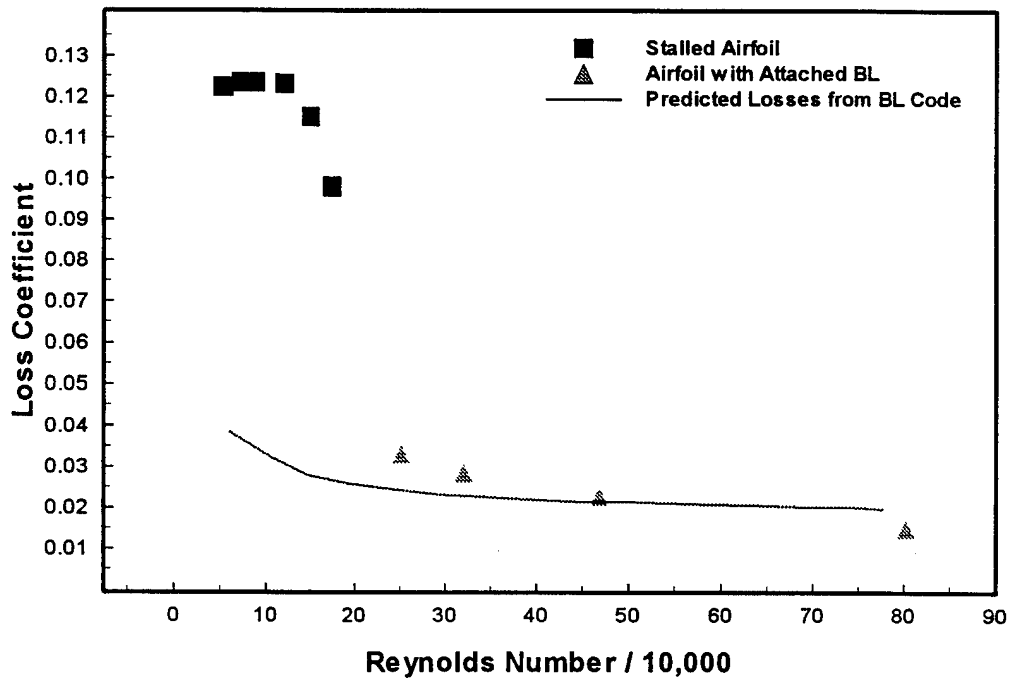

Figure 2. Cascade Losses at Low Reynolds Number (Sharma, 1994)

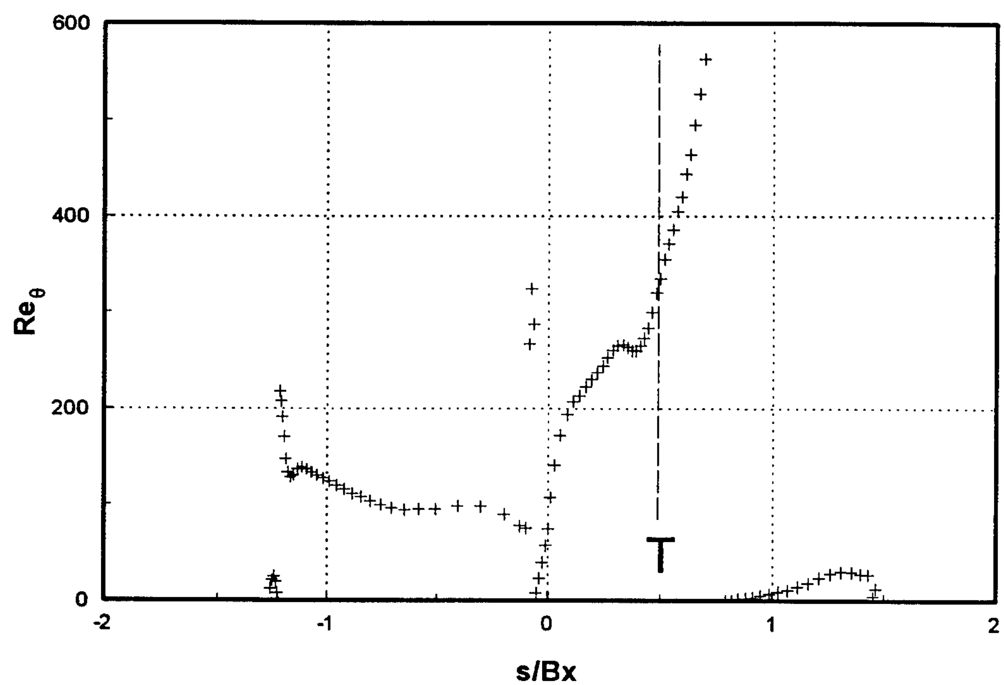

Figure 3. Momentum Thickness Reynolds Number at Transition for a Langston Cascade
Chord Reynolds Number of 50k, C/p = 0.84

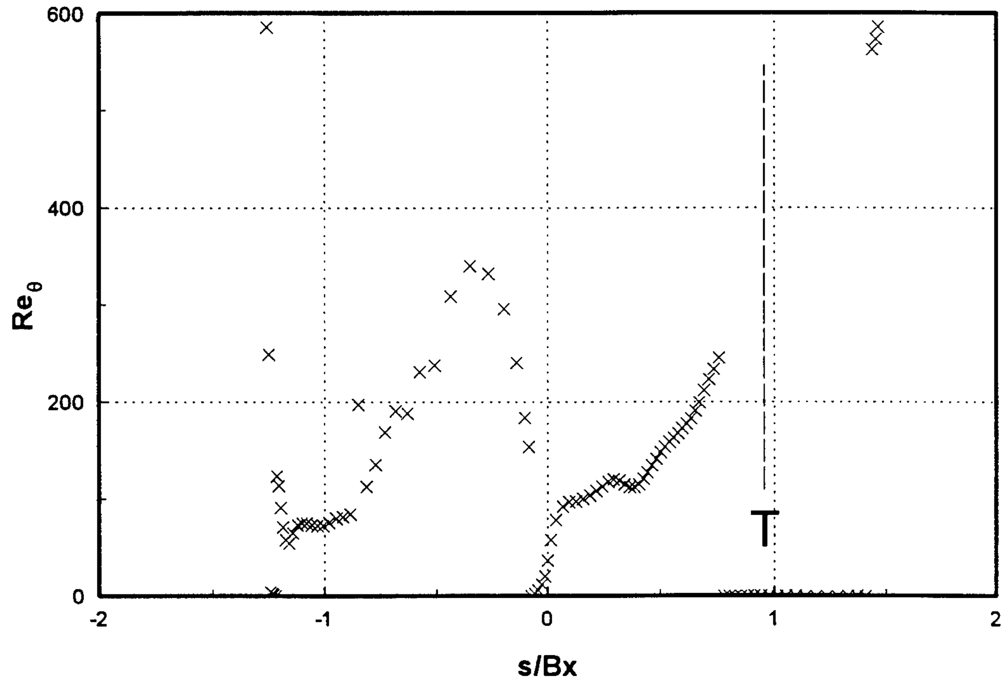

Figure 4. Momentum Thickness Reynolds Number at Transition for a Langston Cascade Chord Reynolds Number of 50k, C/p = 1.075

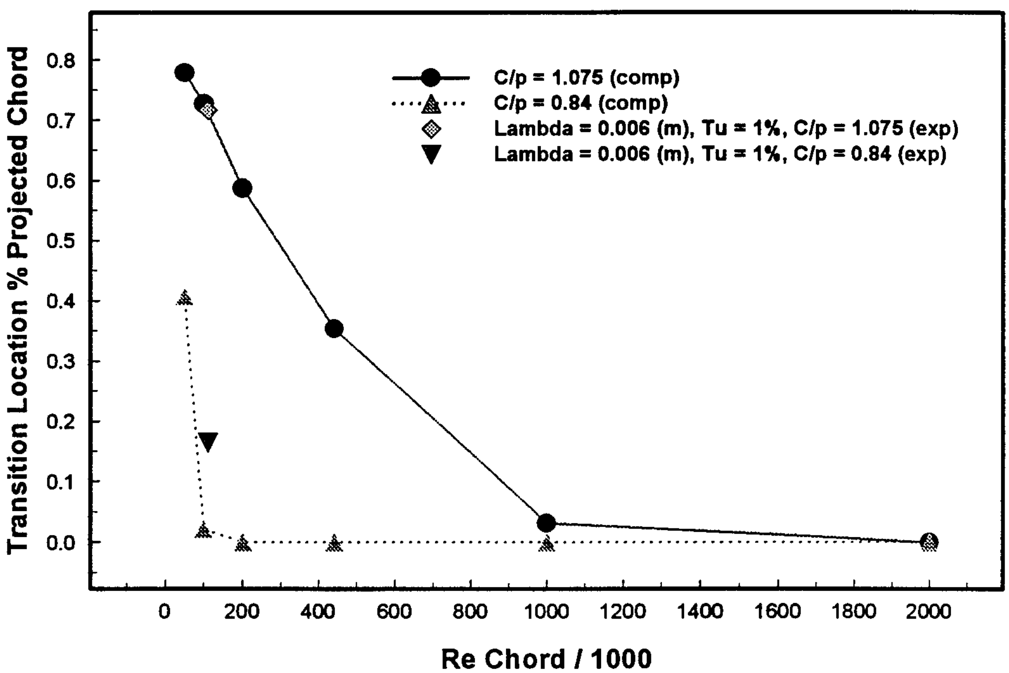

Figure 5. Transition Reynolds Number Dependence in % Projected Chord

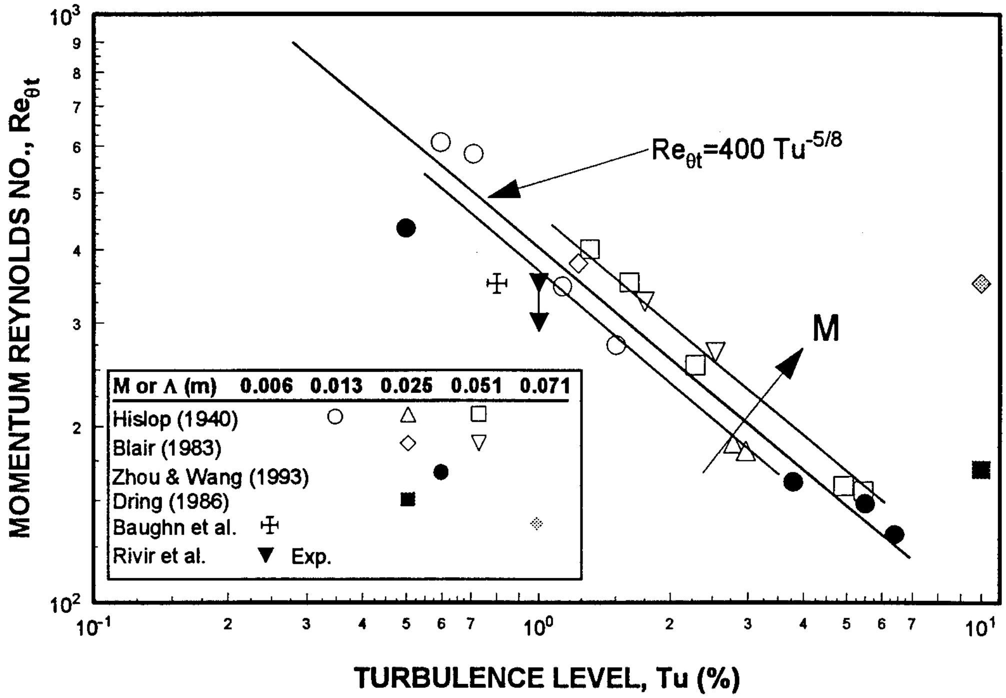

Figure 6. Momentum Thickness Reynolds Number at Transition

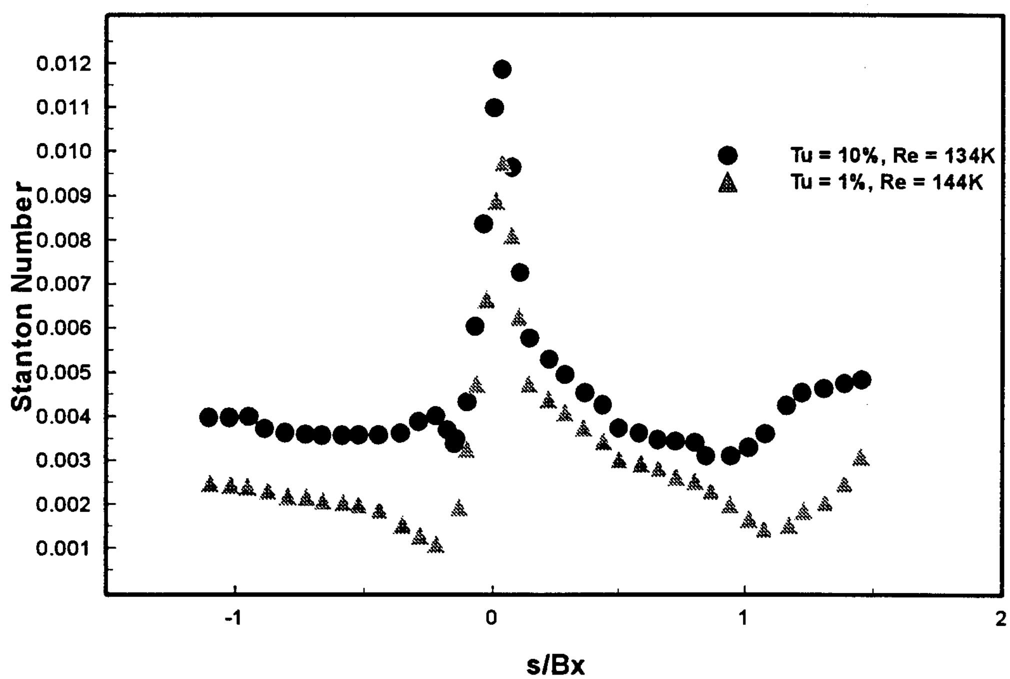

Figure 7. Dependence of Transition Length on Tu

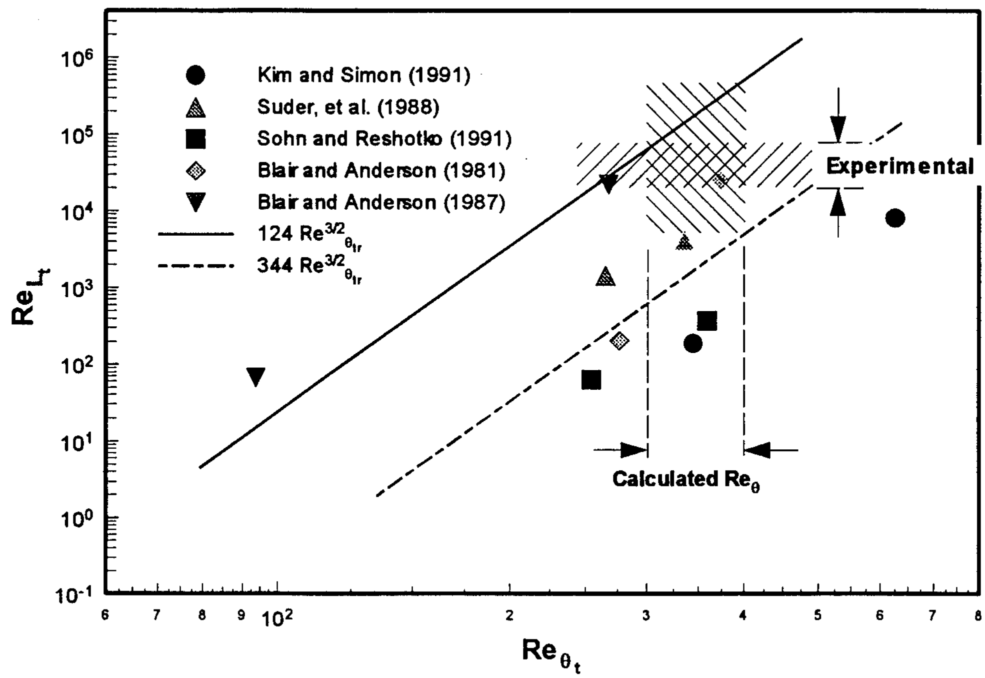

Figure 8. Transition Length Reynolds Number, 0 Pressure Gradient(124), Weak Pressure Gradient(344), (Simon,1994)

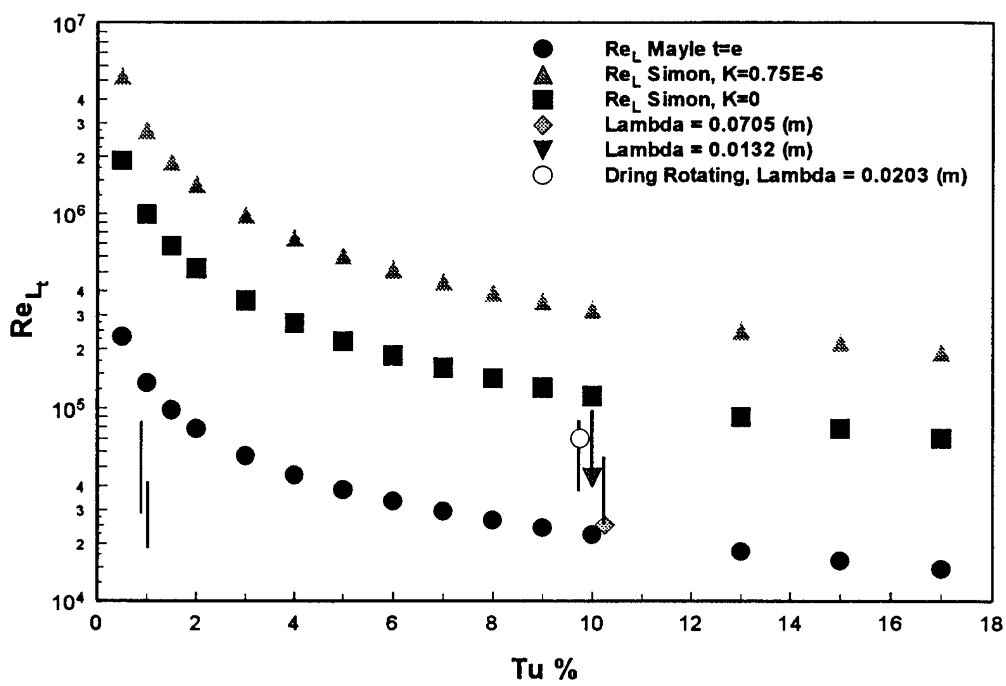

Figure 9. Comparison of Transition Length for 1% and 10% Tu Levels

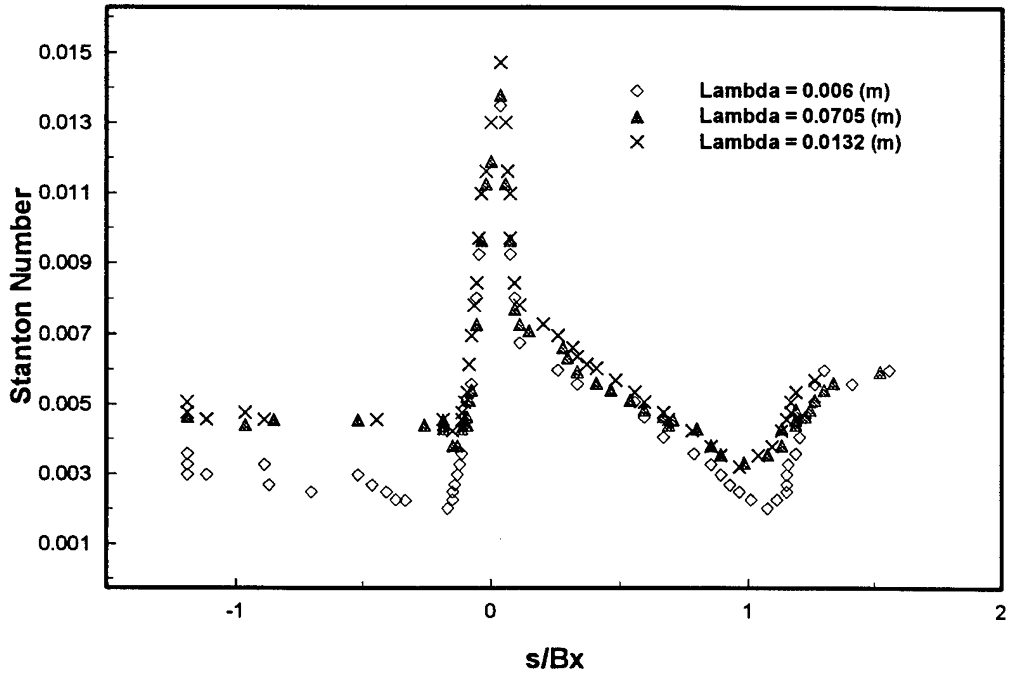

Figure 10. Liquid Crystal Measurements of Transition for Integral Scales 0.0705, 0.0132, (Tu 10%) 0.006 (Tu 0.5%)(Sharp and Harris, 1996)

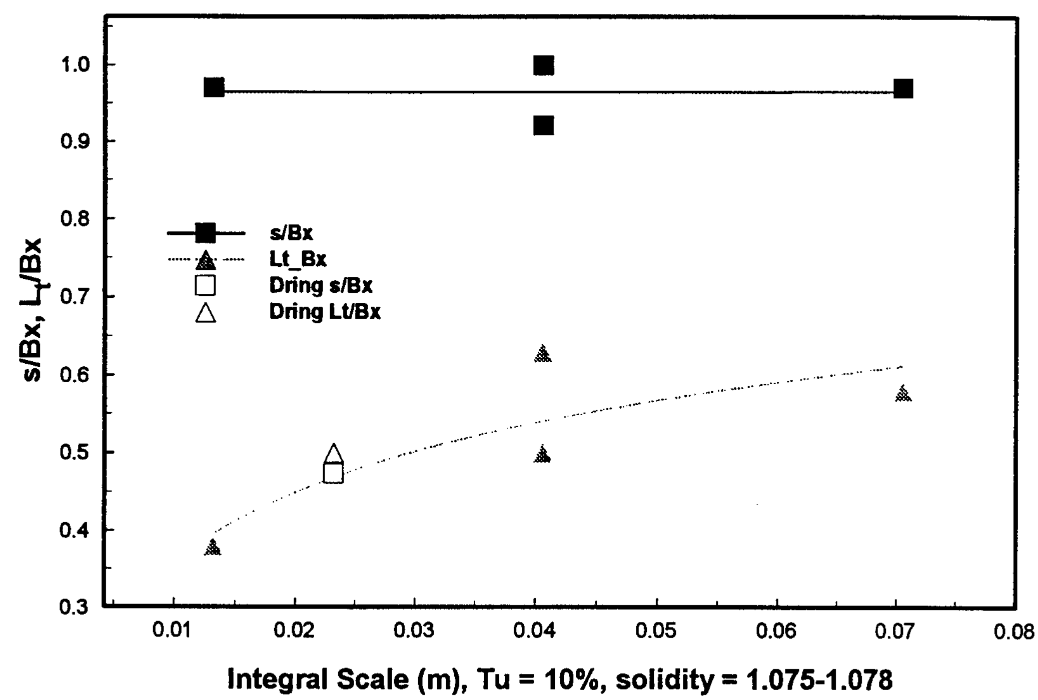

Figure 11. Transition Location and Length in % Projected Chord